Water−Graphite Interaction and Behavior of Water Near the Graphite Surface

Alexander Pertsin and Michael Grunze*

Angewandte Physikalische Chemie, Universität Heidelberg, INF 253, D-69120 Heidelberg, Germany

Received: June 15, 2003; In Final Form: November 10, 2003

Based on MP2 level electronic structure calculations of the binding energy and lowest energy conformation of water−acene complexes [Feller, D.; Jordan, K. D. *J. Phys. Chem. A* **2000**, *104* (44), 9971−9975], three water−graphite model potentials are suggested and tested in grand canonical Monte Carlo simulations of the behavior of water confined between two parallel graphite sheets. It is shown that the thermodynamics and structure of the water−graphite interfacial region are extremely sensitive to the range and orientation dependence of the model potential. This casts doubt on the results of previous molecular dynamics simulations using orientation-independent potentials and standard atomistic force fields. All of the three suggested potentials predict that the water monolayer compressed between two parallel graphite surfaces does not experience capillary evaporation and offers only slight resistance to shear. This explains why water can serve as a lubricant in the friction of graphitic carbons.

1. Introduction

The interaction of water with carbon molecules has attracted considerable attention in recent years. This is partly associated with the practical interest in carbon nanotubes (CNT), which have much promise in biosensor technology and other applications involving water.[1−3] The water−CNT systems have also been the subject of a number of fundamental studies aimed at exploring the structural and phase behavior of water at the nanometer scale.[4] Another reason for the growing interest in the water−carbon interaction has to do with the well-known effect of environmental humidity on the friction and wear of graphitic carbons.[5,6] This effect is usually attributed to the adsorption of water by the third-body layer of aggregated wear debris. It is believed that the adsorbed water acts as a lubricant between the rubbing surfaces of the graphitic particles, thereby enhancing the lubricating properties of the third-body layer. Experimental measurements of the amount of adsorbed water show that water is effective in lubricating carbon−carbon contacts when the water coverage of wear debris is close to a monolayer.[6] This finding, however, is at variance with the common view that graphite is hydrophobic.[7] Once it is hydrophobic, one might expect that water would experience capillary evaporation when confined between graphite surfaces separated by a distance of one or two molecular diameters. Another point to be understood is whether the water monolayer can act as a lubricant between the graphite surfaces. In other words, is the coupling between the water monolayer and the confining graphite surfaces small enough to ensure a negligible shear stress?

The understanding of the water−carbon interaction is of particular importance for computer simulation studies of the water−carbon systems because the results of computer simulations are in general strongly dependent on the model potentials used. In computer simulations, the interaction energy between water and carbon molecules is usually represented as the sum of site−site interactions.[8−14] The interaction sites of the carbon molecule are centered on the carbon atoms, whereas the water molecule is treated in either a single-site (1S) or a three-site (3S) representation, depending on whether the hydrogen atoms are assumed to take part in the interaction. The atom−atom interactions are described by pairwise Lennard-Jones (6−12) potentials. The only exception is the molecular dynamics (MD) simulation of the scattering of water molecules from graphite,[14] where an electrostatic interaction was added between the point quadrupoles on the carbon atoms and the point charges on the water atoms. In a later study,[9] however, the inclusion of the electrostatic term was found to be insignificant.

The 1S-type water−carbon potentials were used in the molecular dynamics (MD) simulations of both the water−CNT and water−graphite systems. Thus Walther et al.[9] and Werder et al.[10] employed the MD technique to simulate the properties of water outside and inside CNT, respectively. The same authors studied the wetting behavior of water on graphite as a function of the carbon−oxygen potential well depth.[8] Hummer et al.[11] simulated the dynamics of water inside CNT and observed unusual pulselike transmission of water molecules through CNT. One more MD simulation of the water−CNT system based on the 1S water−carbon potential was reported by Koga et al.,[12] who found the formation of ordered ice nanotubes inside CNT. The 3S water−carbon potential was employed in the MD simulation of the water−CNT system by Noon et al.,[13] where the ordering of water inside CNT into helical ice sheets was observed. Another application of this potential was reported by Werder et al.,[8] who simulated the water contact angle on graphite for three selected sets of the potential parameters.

The parametrization of the available water−carbon potentials has been recently reviewed by Werder et al.[8] The weakness common to all parametrizations is, in our view, an overestimated transferability of the potentials between different systems. This refers, for instance, to the molecular water−carbon potential used in refs 9, 10, and 14, where the O···C atom−atom interaction parameters were borrowed from the Bojan−Steele potential[15] derived from the adsorption of molecular oxygen on graphite. In other words, it was implicitly assumed that the oxygen atoms in water and in molecular oxygen are similar, which is certainly not so in view of a very specific behavior of water in the intermolecular interactions. The same criticism applies to the water−carbon potentials constructed on the basis of "universal" force fields such as CHARMM[16] and AM-

* To whom correspondence should be addressed.

10.1021/jp0356968 CCC: $27.50
Published on Web 12/20/2003

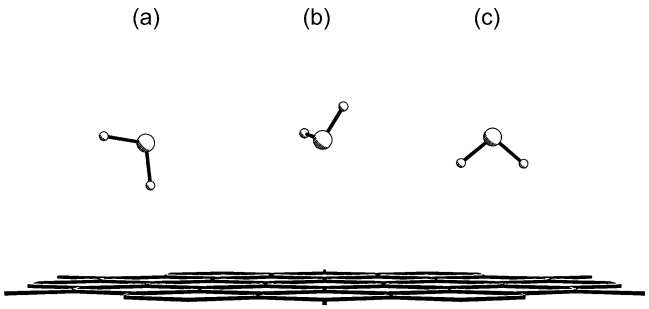

Figure 1. Equilibrium orientation of a water molecule near graphite surface: (a) MP2 level ab initio calculation;[18] (b) 1S model potential; (c) 3S model potential with parameters from CHARMM force field.[16]

BER96,[17] whose calibration included no system where the specific water−carbon interactions could be probed.

In view of surprisingly little experimental data on the interaction of water with carbon molecules, of great significance are the relevant ab initio electronic structure calculations. Quite recently, Feller and Jordan[18] have published MP2 level ab initio results for the interaction of a water molecule with a series of acenes up to $C_{96}H_{24}$. The estimated binding energy of the water molecule to single-layer graphite proved to be $\Delta E = -5.8 \pm 0.4$ kcal/mol, which is substantially lower than the model potential predictions ranging from −1.7 to −4.3 kcal/mol.[19,20] Moreover, the ab initio estimate for ΔE is about twice as low as the threshold value of ΔE for a complete wetting of graphite by water ($\Delta E \approx -3$ kcal/mol), as found in the MD simulations of a water droplet on graphite[8] for a number of 1S-type and three 3S-type (6−12) potentials. That is, according to the MD simulation results,[8] the ab initio estimate $\Delta E = -5.8$ kcal/mol is at variance with the experimental observation of nonvanishing water contact angles on graphite.[21−24] On the other hand, it is important to note that the threshold of $\Delta E = -3$ kcal/mol was derived in the MD simulations[8] using a very restricted range of potential types, and so it cannot be generalized to potentials of another form. It will be shown in the following that the thermodynamics of the water−graphite interface are not uniquely determined by the magnitude of ΔE. Examples will be presented of how different water−graphite potentials with exactly the same ΔE may well result in quite different interfacial tensions and wetting behavior.

Another disagreement of the ab initio MP2 calculation results[18] with the predictions of the model potentials concerns the preferred orientation of the water molecule near the graphite surface. According to the lowest energy water−acene conformation found in the ab initio calculations,[18] a water monomer forms a kind of single hydrogen bond with graphite, with one OH bond pointed toward the graphite surface, as shown in Figure 1a. None of the water−graphite model potentials available in the literature can, however, reproduce such an orientation. Thus, the 1S water−graphite potential depends only on the O···C separation and it cannot distinguish between different water orientations at all, regardless of the potential parameters used. (This is illustrated in Figure 1b by showing the water molecule in some arbitrary orientation.) The 3S potential is orientation dependent, but the water orientations predicted with the available parameter sets have little to do with that found in the ab initio MP2 calculation.[18] For example, the model potential based on the CHARMM force field[16] predicts a symmetric water orientation, with the water dipole moment directed perpendicularly to the graphite surface (Figure 1c). A similar orientation is predicted by the Marcović et al.[14] model potential that includes the electrostatic charge−quadrupole terms. The other available potentials of the 3S type result in preferable orientations which differ from the symmetric one by a tilt of the HOH plane.

In our recent Monte Carlo simulation[25] of the behavior of water near model solid surfaces, we have found that the orienting effect of the surface on the adjacent water molecules has a profound influence on the structure and energetics of the water−solid interface. In view of this finding, the inability of the available model potentials to describe the orientation dependence of the water−carbon interaction makes questionable the intriguing results of the recent MD simulations[11−13] concerning the structure and dynamics of the water−CNT systems.

In the present work, we consider three trial water−graphite potentials, one of the 1S type and the other two of the 3S type. All three potentials well reproduce the MP2 calculation results for ΔE and the equilibrium separation of water from the graphite surface. In addition, the 3S-type potentials both recover the MP2 prediction for the equilibrium orientation of the water molecule with respect to the surface normal. The three potentials are tested in grand canonical Monte Carlo (GCMC) simulations of the behavior of water confined between two parallel single-layer graphite sheets. The simulation results are compared with the little that is known experimentally about the thermodynamics of the water−graphite interaction. The shear behavior of water confined between the graphite surfaces is also explored to gain a better understanding of the effect of water on the friction and wear of graphitic carbons.

2. Method

2.1. Interaction Potentials. As repeatedly discussed in the literature,[26,27] the treatment of the interaction of molecules in terms of the interaction of their constituent atoms is quite a rough approximation, which suffers from a few conceptual drawbacks and which has received wide use mainly for the reason of computational simplicity. The associated atom−atom potentials do not have exact physical meaning and can be rather regarded as certain "basis" functions in an analytical representation of the true intermolecular potential. With this consideration in mind, we treated the atom−atom potential parameters in a purely formal way, ignoring, for example, the intuitive view that the O···C atom−atom interaction should be stronger than the H···C one and hence the O···C potential well depth should be larger than that of the H···C potential. To keep the water−graphite interaction model computationally inexpensive, we restricted ourselves to inverse power atom−atom potentials

$$\varphi_{m-n}(r) = \frac{\epsilon}{n-m}\left[m\left(\frac{d}{r}\right)^n - n\left(\frac{d}{r}\right)^m\right] \quad (m \geq 6, n > m) \quad (1)$$

where ϵ and d are the depth and position of the potential well, respectively. No explicit orientation-dependent terms were incorporated in the total water−graphite potential. The orientation dependence arose in 3S-type potentials just due to the presence of three different force sites on the water molecule.

All the atom−atom potentials were used in the energy-shifted form:[28]

$$\varphi(r) = \begin{cases} \varphi_{m-n}(r) - \varphi_{m-n}(r_c), & r < r_c \\ 0, & r \geq r_c \end{cases} \quad (2)$$

where r_c is the cutoff radius. The magnitude of r_c was taken to be 7.2 Å, which is equal to that used in calculating the Lennard-Jones contribution to the water−water interaction energy. That is, the range of the water−wall interaction included only two hydration layers near the graphite surface. For comparison, a cutoff of 10 Å was also tested. The associated changes in the lowest energy conformation of the complex proved to be

TABLE 1: O···C and H···C Atom−Atom Potential Parameters Fitted To Reproduce Binding Energy and Lowest Energy Conformation of Water/Single-Layer Graphite Complex

model	d_{OC}, Å	ϵ_{OC}, kcal/mol	m_{OC}	n_{OC}	d_{HC}, Å	ϵ_{HC}, kcal/mol	m_{HC}	n_{HC}
1S	3.645	0.450	6	12				
3Sa	3.85	0.184	6	12	2.143	1.105	8	12
3Sb	3.9	0.093	8	14	2.2	1.988	10	16

insignificant, whereas the observed increase in ΔE could be easily compensated for by the respective scaling of the potential well depths. For a 1S-type (6−12) potential, for example, the increase in ΔE on going from $r_c = 7.2$ Å to $r_c = 10$ Å could be recovered by a ∼15% increase in the O···C well depth, while keeping r_c at 7.2 Å.

The parametrization of the water−graphite potential was made using a trial-and-error procedure, by testing various sets of potential parameters in recovering the asymmetric conformation of the water−single-layer graphite complex, as depicted in Figure 1a. (Recovering $\Delta E = -5.8$ kcal/mol involved no difficulties—this could be easily done by scaling the potential well depths ϵ_{OC} and ϵ_{HC}.)

The test of a trial potential involved minimization of the interaction energy of the water−graphite complex as a function of three translational and three rotational parameters describing the position and orientation of the water molecule over the graphite surface. A lowest energy conformation was regarded as acceptable if the deviation of the O−H bond direction from the surface normal did not exceed 15° and the separation of the water oxygen atom from the graphite surface, h_O, was between 3.0 and 3.2 Å. Inasmuch as the focus of our work was on the effect of the orientation dependence of the potential, no attempt was made to reproduce the MP2 prediction for the lateral position of the water molecule. Initially, we tried to describe the O···C and O···H atom−atom interactions using Lennard-Jones (6−12) potentials. It turned out, however, that the required asymmetric conformation of the water−graphite complex was better reproduced with shorter ranged potentials, particularly for the H···C interaction.

As is typical of parameter fittings based on a limited database, the solution of the parametrization problem was not unique: There existed a number of parameter sets which reproduced the MP2 results equally well. To make the choice of potential parameters more definite, we imposed additional requirements upon the water−graphite potential, based on the GCMC simulations of water in contact with graphite. Unfortunately, the experimental data on the thermodynamics of the water−graphite interface are very limited and contradictory. Thus, the reported values for the water contact angle on graphite, θ, range from 30° to 86°.[21−24] The large uncertainty seems to originate from a high sensitivity of θ to the cleanness of the graphite surface. In view of this uncertainty, the associated requirement was taken to be rather soft; viz., we only assumed that the water wetting of graphite should be partial, that is, $(\gamma_{sv} - \gamma_{sl})/\gamma_{lv} < 1$, where the subscripts s, l, and v at the interfacial tensions γ refer, as usual, to the solid, liquid, and vapor phases, respectively. This inequality imposes a lower limit upon the water−graphite interfacial tension, $\gamma_{sl} > \gamma_{sv} - \gamma_{lv}$. Here again, whereas the surface tension of water is known with certainty ($\gamma_{lv} = 72$ dyn/cm), the available literature values for the surface tension of graphite γ_{sv}, derived mostly from estimates for the interlayer binding energy, differ by 2 orders of magnitude, ranging from 6 to 600 dyn/cm (see ref 29 for a brief review). The most recent (and probably most reliable) estimate for γ_{sv} is 110^{+50}_{-30} dyn/cm, as obtained from the balance of the curvature energy and the interlayer attraction for a simple elastic model of a collapsed carbon nanotube.[29] On the basis of the above-discussed experimental data, we can accept that a correct water−graphite potential should predict a positive water−graphite interfacial tension γ_{sl}, with a magnitude on the order of several tens of dynes per centimeter.

Whereas the available estimates for θ and γ_{sv} point to a limited water affinity of the graphite surface, the observation of stable water films of monolayer thickness between graphite particles[6] suggests that the water affinity of graphite is high enough to prevent the water films from capillary evaporation. The existence of these mutually opposite conditions provides a good test for the water−graphite model potential.

Because of the high computational cost of GCMC simulations, our test was restricted to three model potentials, whose parameters are listed in Table 1. The parameters correspond to $\Delta E = -5.8$ kcal/mol, but they can be easily modified to reproduce any desired ΔE by appropriately scaling the well depths. The 1S potential in Table 1 is of the usual Lennard-Jones form. Its well position d_{OC} was borrowed from Jaffe's 1S potential,[30] which was quoted by Werder et al.[8] as the one that reproduced the MP2 prediction for ΔE. The value quoted for ϵ_{OC} (0.31 kcal/mol)[8] is, however, noticeably less than our result. One possible reason is that our calculations use the atom−atom potentials in the energy-shifted form, as given by eq 3. Because of the presence of a positive energy shift of $-\varphi_{m-n}(r_c)$, our model potential requires a larger ϵ_{OC} to reproduce the same ΔE. The necessary increase in ϵ_{OC} is obviously larger the smaller the cutoff radius, r_c. Another possible reason for the difference in ϵ_{OC} between our model and Jaffe's[30] model is that the latter seems to refer to the graphite crystal and not a single layer as in our work. Inasmuch as the second and deeper graphite layers make a perceptible contribution to the water−graphite binding energy (∼0.6 kcal/mol for the Jaffe potential), the same ΔE can indeed be reproduced with a smaller ϵ_{OC}.

In addition to recovering the MP2 prediction for ΔE, the three-site models 3Sa and 3Sb in Table 1 both reproduce the asymmetric orientation of the water molecule, with one OH bond pointed toward the graphite surface (Figure 1a). The orientation behavior of the 3Sa model can be appreciated from Figure 2, which shows the interaction energy of a water molecule with a

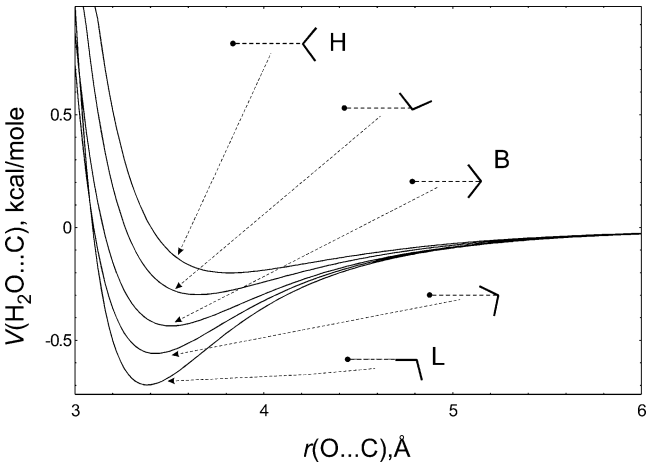

Figure 2. Interaction energy of a water molecule with a single carbon atom, as a function of O···C separation for some selected water orientations. Labels L, B, and H refer to the lowest energy, "bifurcated", and the highest energy conformers, respectively.

single carbon atom, $V(H_2O\cdots C)$, as a function of the O···C separation for some selected water orientations. The preference of the linear O−H···C conformer is clearly seen. It is worth noting that the potential well depth of $V(H_2O\cdots C)$ in the linear configuration (∼0.7 kcal/mol) is perceptibly smaller than ϵ_{HC} (see Table 1). The reason is that the region of the H···C potential minimum is overlapped with the repulsive wing of the O···C potential, and it is this overlap that makes the linear C···H−O configuration most favorable: Any deviation from linearity increases the overlap and makes the C···H−O interaction more repulsive.

The orientation dependence of $V(H_2O\cdots C)$ for the 3Sb model is qualitatively similar but much stronger. This can be appreciated in terms of reduction in the well depth of $V(H_2O\cdots C)$ on going from the lowest energy conformer L to the "bifurcated" conformer B and then to the highest energy conformer H (see Figure 2 for notations). For model 3Sa, the respective well depths are related as $\epsilon_L:\epsilon_B:\epsilon_H = 1:0.6:0.3$, whereas model 3Sb predicts $\epsilon_L:\epsilon_B:\epsilon_H = 1:0.3:0.1$. The reason for the use of a water−graphite potential with a stronger orientation dependence will be clear from the discussion of the simulation results in section 3.

The equilibrium separation of the water oxygen atom from the graphite surface is $h_O = 3.1$ and 3.0 Å for models 3Sa and 3Sb, respectively, which is somewhat shorter than the MP2 result ($h_O = 3.2$ Å).[18] It should, however, be noted that the MP2 prediction for h_O is based on the geometry optimization for a fairly small acene molecule, $C_{18}H_{12}$, comprising only four fused rings. Considering the observed increase in the magnitude of ΔE with increasing number of fused rings, a concomitant slight decrease in h_O cannot be ruled out.

Another difference between the MP2 and 3S model predictions has to do with the lowest energy lateral position of the water molecule over the graphite surface. Using the terminology of hydrogen bonding, this difference can be referred to as the difference in the arrangement of the "proton acceptor sites" on the graphite surface. According to the MP2 calculation,[18] the water molecule forms a nearly linear hydrogen bond with a carbon atom; i.e., the lattice of proton acceptor sites coincides with the lattice of carbon atoms in the graphite sheet. By contrast, the 3S model potentials predict that the hydrogen bond is formed between the water molecule and the center of a six-membered ring. (This is not unexpected as far as the H···C interaction is described by isotropic potentials, which tend to maximize the number of carbon atoms around the hydrogen atom.) The respective lattice of proton acceptor sites is crystallographically identical to the lattice of next nearest carbon atoms, with a surface density twice as low as that of all carbon atoms. We are not inclined to give much importance to this difference insofar as two nearest carbon atoms in the graphite sheet are too close together to be occupied by two water molecules at a time. The separation between the next nearest atoms is 2.47 Å, so they can accommodate two water molecules with only small displacements (0.1−0.2 Å) from their lowest energy positions. In this respect, the MP2[18] and model predictions for the lattice of proton acceptor sites are equivalent. It should also be noted that for the 3S model potentials the energy difference between the MP2 and model sites is as small as 0.4 kcal/mol, i.e., less than kT. That is, in a computer simulation at room temperature the two different proton acceptor sites are practically indistinguishable for the water molecule.

In the computer simulations of the behavior of water confined between graphite sheets, the water−graphite potentials with parameters from Table 1 were combined with the well-known TIP4P model for water.[31] As already mentioned above, the Lennard-Jones part of the water−water potential was cut off at 7.2 Å. The electrostatic interactions were smoothly damped in the range between 7 and 7.5 Å using a switching function suggested by Lee and Rossky.[32] The direct interaction between the confining graphite sheets was estimated using the (6−12) atom−atom C···C potential suggested by Crowell ($\epsilon_{CC} = 0.0556$ kcal/mol, $d_{CC} = 3.82$ Å).[33] This interaction was significant only at the shortest wall-to-wall separations, where it added about 2 kbar to compressional stress.

2.2. Simulation Procedure. The simulated system represented a slab of water confined between two parallel single-layer graphite sheets and allowed to exchange molecules with a fictitious bulk water reservoir. The chemical equilibrium between the confined and bulk water was maintained using the GCMC technique. The excess (nonideal) part of the chemical potential was taken to be −6.1 kcal/mol, which best reproduced the properties of bulk water under ambient conditions for the water model and summation scheme used.[25] The simulation procedure was basically the same as described in our previous publications.[25,34,35] The confining graphite layers were treated as rigid, so the water−graphite interaction could be considered as an external field. To improve the efficiency of insertions and deletions, the excluded volume mapping method[36] and a Swendsen−Wang filter[37] based on evaluation of the van der Waals energy of the system were employed.

The simulation box was taken to be a rectangular prism with lateral dimensions L_x and L_y and height h. The lower and upper graphite sheets were placed at $z = 0$ and $z = h$ parallel to the $x-y$ plane. In the x and y dimensions, the system was replicated periodically. To conform to the periodic boundary conditions, L_x and L_y were taken to be multiples of the graphite lattice periods $a = 3l$ and $b = \sqrt{3}l$, where l is the CC bond length in graphite (1.426 Å). The particular dimensions used were $L_x = 8a = 34.2$ Å and $L_y = 13b = 32.1$ Å. With this choice, each graphite sheet contained 416 carbon atoms.

A typical GCMC run comprised 3×10^6 passes, each composed of N moves, where N is the current number of water molecules. The first 0.5×10^6 passes were discarded to allow for equilibration of the system. For the largest systems studied ($N \sim 700$), a total of 2×10^9 configurations were attempted.

The effect of the graphite walls on the structure and energetics of the adjacent water was analyzed in terms of the z profiles of various quantities and functions, including the average water density, pair distribution functions in planes parallel to the wall, $x-y$ density maps, orientational distributions of the water OH bonds and dipole moments, average interaction energies of a water molecule with surrounding water molecules and the walls, and others. To this end, the simulation box was divided into slices 0.1−0.2 Å thick, lying parallel to the walls. During the GCMC run, the z-dependent quantities were averaged within each individual slice and then referred to the z coordinate of its center.

In addition to the ensemble averaged potential energy $\langle U\rangle$ and number of molecules $\langle N\rangle$, we evaluated the z-averaged normal and tangential components of the Irving−Kirkwood pressure tensor $P_{\alpha\beta}$ ($\alpha, \beta = x, y, z$).[38] The normal component was calculated from the equation

$$P_N = \bar{P}_{zz} = \frac{1}{Ah}\left\langle NkT - \sum_i \left[\frac{1}{2}\sum_{j\neq i}\sum_{a\in i,b\in j} z_{ij}z_{ab}\varphi'_{ab}(r_{ab})/r_{ab} + \sum_{a\in i,c} z_i z_a \varphi'_{ac}(r_{ac})/r_{ac} + \sum_{a\in i,c'} (h - z_i)(h - z_a)\varphi'_{ac'}(r_{ac'})/r_{ac'}\right]\right\rangle \quad (3)$$

In this equation, $A = L_xL_y$ is the cross-sectional area of the

simulation cell in the $x-y$ plane; indices i and j run over the water molecules, a and b run over the force sites in molecules i and j, and c and c' run over the carbon atoms in the lower and upper graphite sheets, respectively; $z_{ab} = z_a - z_b$, $\mathbf{r_{ab}} = |\mathbf{r}_a - \mathbf{r}_b|$, $z_{ij} = z_i - z_j$, where the coordinates z_i and z_j refer to the centers of mass of molecules i and j; φ_{ab} and φ_{ac} are the site−site interaction potentials. If the water−graphite potential is treated as an external field due to a rigid graphite lattice, the equation for the tangential pressure P_T can be shown to contain only terms due to the water−water interactions:

$$P_T = \frac{1}{2}(\bar{P}_{xx} + \bar{P}_{yy}) = \frac{1}{Ah}\left\langle NkT - \frac{1}{4}\sum_i \sum_{j\neq i} \sum_{a\in i, b\in j} (x_{ij}x_{ab} + y_{ij}y_{ab})\varphi'_{ab}(r_{ab})/r_{ab} \right\rangle \quad (4)$$

The knowledge of P_T along with the bulk pressure P_b allows evaluation of the tension of the confined water film:

$$\gamma(h) = (P_b - P_T)h \quad (5)$$

which is related to the water−graphite interfacial tension γ through the limiting expression:

$$\gamma(h) \to 2\gamma \quad \text{at} \quad h \to \infty \quad (6)$$

In the analysis of the shear behavior of the system, we followed the "quasistatic" approach,[39−42] assuming the shear rate to be much lower than the rate of the molecular relaxation processes in the system, as it actually occurs in nanotribological studies using surface-force apparatus and atomic-force microscopes. With this assumption, the shear can be regarded as a succession of equilibrium states, each associated with a particular lateral alignment of the confining walls. That is, unlike MD simulations of the rheological properties of confined liquid films,[43−45] quasistatic Monte Carlo simulations contain no shear rate. A critical comparison of the quasistatic and dynamic approaches can be found in a review article by Bordarier et al.[39]

In the present simulations, we consider shear strains α applied along the y axis, so that the positions of the carbon atoms in the upper and lower walls are related by the equations

$$x_{c'} = x_c \quad (7)$$

$$y_{c'} = y_c + \alpha b \quad (8)$$

$$z_{c'} = z_c + h \quad (9)$$

The shear stress T_{zy} conjugate to α was calculated in the "force" form through the ensemble averaged force acting on the upper wall

$$\langle F_y \rangle = \sum_i \sum_{a\in i, c'} y_{ac'}\varphi'_{ac'}(r_{ac'})/r_{ac'} \quad (10)$$

$$T_{zy} = \langle F_y \rangle / A \quad (11)$$

where $\langle F_y \rangle$ is the y component of the ensemble averaged force acting on the upper wall.

To improve statistical accuracy, the force on the lower wall $\langle F_y \rangle_{\text{lower}} = -\langle F_y \rangle_{\text{upper}}$ was also evaluated, and T_{zy} was calculated as the average:

$$T_{zy} = (\langle F_y \rangle_{\text{upper}} - \langle F_y \rangle_{\text{lower}})/2A \quad (12)$$

3. Results and Discussion

We started our GCMC simulations with a comparison of models 1S and 3Sa in describing the properties of the water−graphite interface. The initial objective was to see the manifestations of the orienting effect of the water−wall interaction potential in the structure, thermodynamics, and shear behavior of the system. To analyze the influence of a single graphite wall on the structure and energetics of the adjacent water layers, we first simulated the behavior of the system at a wall-to-wall separation $h = 40$ Å, which is large enough to neglect the joint effect of the opposite walls.

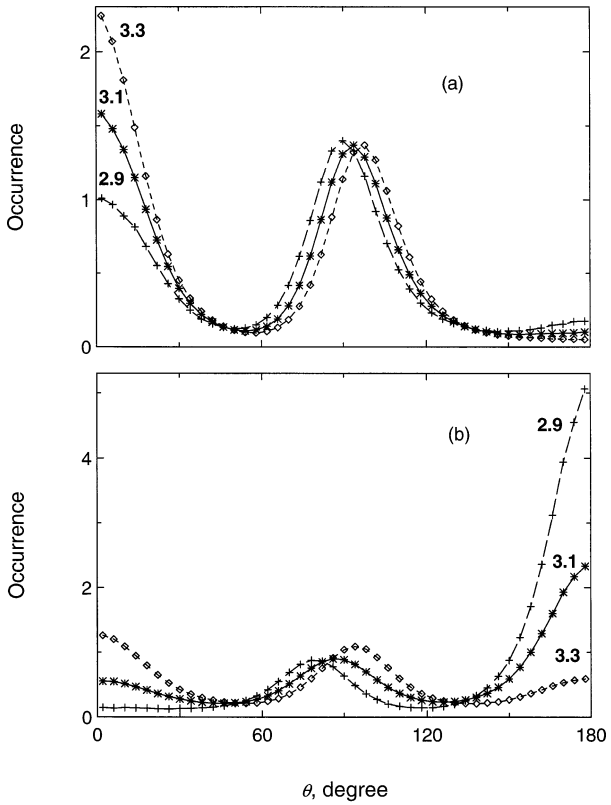

Figure 3. Orientational distribution of water molecules in the first hydration layer near graphite surface for (a) 1S model potential and (b) 3Sa model potential. The numbers at the curves indicate the separation of water molecules from the graphite substrate in angstroms.

Although the 1S model potential contains no explicit orientation-dependent terms, the 1S model wall does have a perceptible orienting effect on the neighboring water molecules. This can be seen from Figure 3a, which shows the distribution of angles θ formed by the OH bond vector and the z axis. The data refer to three slices in the separation range from 2.9 to 3.3 Å, i.e., within the first hydration layer. In the preferred orientation, the water molecule has one OH bond pointed outward the graphite surface ($\theta = 0$). The preference for this orientation can be attributed to the trend of the water molecules to maximize the number of hydrogen bonds with their neighbors, which is achieved by minimizing the number of OH bonds oriented toward the graphite surface. A similar orientational distribution of water was found near nonorienting structureless[25] and atomistic[9] walls. Quite the reverse situation is observed with the 3Sa model wall, which favors hydrogen bonding orientations with one OH bond pointed toward the wall ($\theta = 180°$, see Figure 3b). We may thus conclude that the assumed orientational dependence of the 3Sa model potential is strong enough to induce the respective orientational order in water adjacent to the model wall.

As seen from Figure 4, the 1S and 3Sa models generate markedly different water density profiles in the interfacial region despite the same binding energy ΔE. The orienting wall results in much lower density maxima, indicative of a less hydrophilic

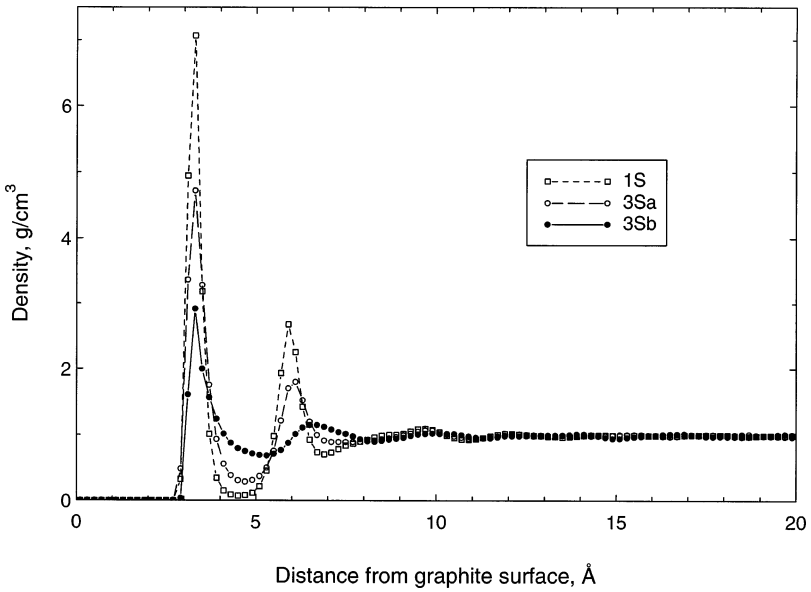

Figure 4. Water density profiles near graphite surface, as simulated using 1S, 3Sa, and 3Sb model potentials for the water−graphite interaction.

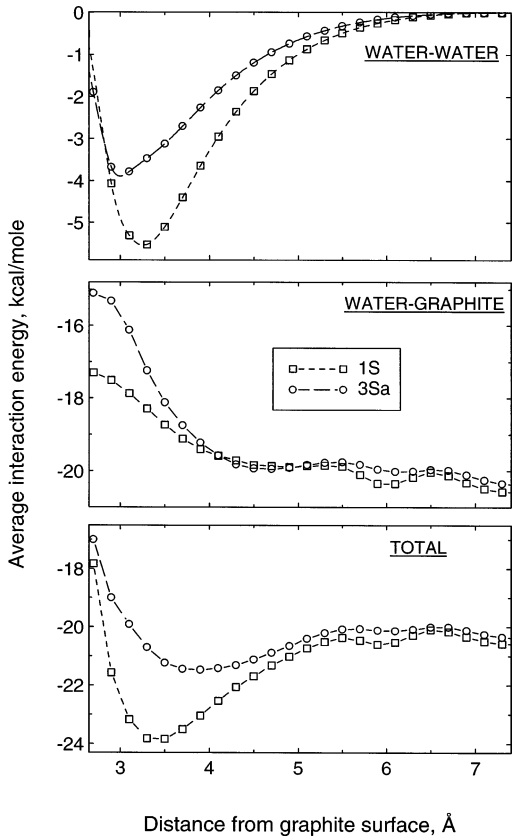

Figure 5. Average interaction energy of a water molecule with its surroundings and individual contributions to this energy for 1S and 3Sa models.

surface. The lower hydrophilicity of the 3Sa wall can also be inferred from Figure 5, which presents the average interaction energy of a water molecule with its surroundings as a function of the separation from the wall. Both the total interaction energy and its constituents due to the water−water and water−wall interactions are shown. One can see that the residence of a water molecule near the 3Sa wall is energetically less favorable, compared to the 1S wall. The reason is that the trend of the 3Sa wall to form hydrogen bonds with the neighboring water molecules interferes with the trend of the water molecules to form hydrogen bonds with themselves. As a consequence, there is a noticeable loss in both the water−wall and water−water contributions to the average interaction energy, as compared to the nonorienting wall with the same ΔE.

With both the 1S and 3Sa models, the confined water film did not experience capillary evaporation down to thicknesses corresponding to one water monolayer. The behavior of water at small wall-to-wall separations h was typical of molecularly thin liquid films. Due to the tendency of confined water molecules to arrange themselves in layers parallel to the walls, the normal pressure P_N was an oscillating function of h, with a period close to the molecular diameter of water. The dependence of P_N on h in the range $6.2 \leq h \leq 11$ Å is depicted in Figure 6 for model 3Sa. The regions of positive and negative P_N refer to compressed and stretched water films, respectively. In the context of the effect of water on the frictional properties of graphite, our interest is in the shortest separations ($h < 6.7$ Å) corresponding to a compressed water monolayer.

The shear behavior of the compressed monolayer film can be appreciated from Figure 7, which shows the shear stress T_{zy} as a function of registry α for three different separations h. Considering that the function $T_{zy}(\alpha)$ is antisymmetric with respect to $\alpha = 0$, we show only a symmetrically independent part of $T_{zy}(\alpha)$ in the interval $0 \leq \alpha \leq 0.5$. In can be seen that the simulation predicts the existence of some tangential coupling between the water monolayer and the confining graphite sheets. The coupling is, however, weak, so the observed magnitudes of the yield stress $T_{zy}^c = \max\{T_{zy}(\alpha)\}$ are substantially less than the respective normal pressures. Estimates of the static friction coefficient as the ratio T_{zy}^c/P_N range from 0.01 to 0.02, which is more than an order of magnitude lower than the friction coefficient of graphite in a vacuum (0.5−0.8). For model 1S, the simulation results for P_N and T_{zy} at monolayer thicknesses were not too different from those for model 3Sa (see Figure 7 for P_N), so the friction coefficient was of the same order of magnitude. Considering that the loss of lubrication properties by molecularly thin films is frequently associated with solidification of confined liquid,[46] we note that the water monolayer confined between graphite surfaces remained liquidlike at all relevant h, as judged from the form of the pair distribution functions.

Although both the 1S and 3Sa models successfully predict that a stable water monolayer can exist between graphite surfaces and can well serve as a lubricant in the friction process, both

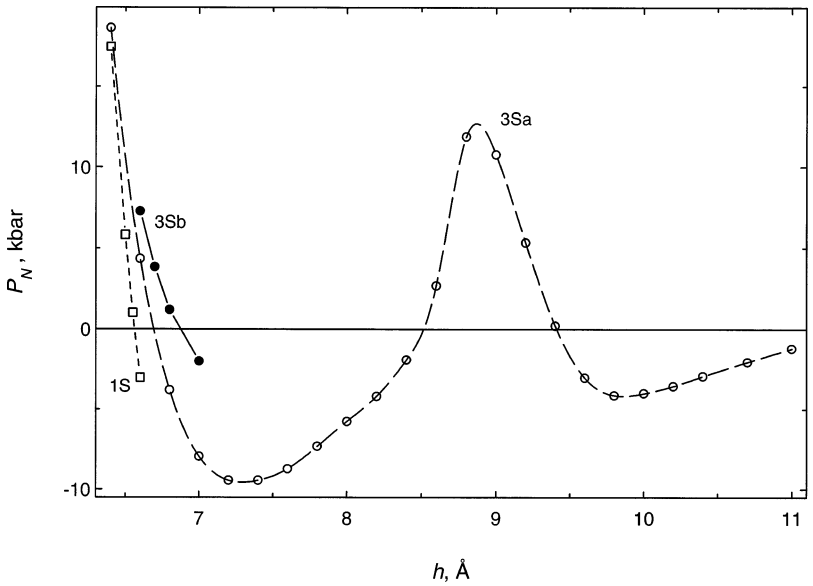

Figure 6. Normal pressure as a function of wall-to-wall separation, as calculated using 1S, 3Sa, and 3Sb model potentials for water−graphite interaction.

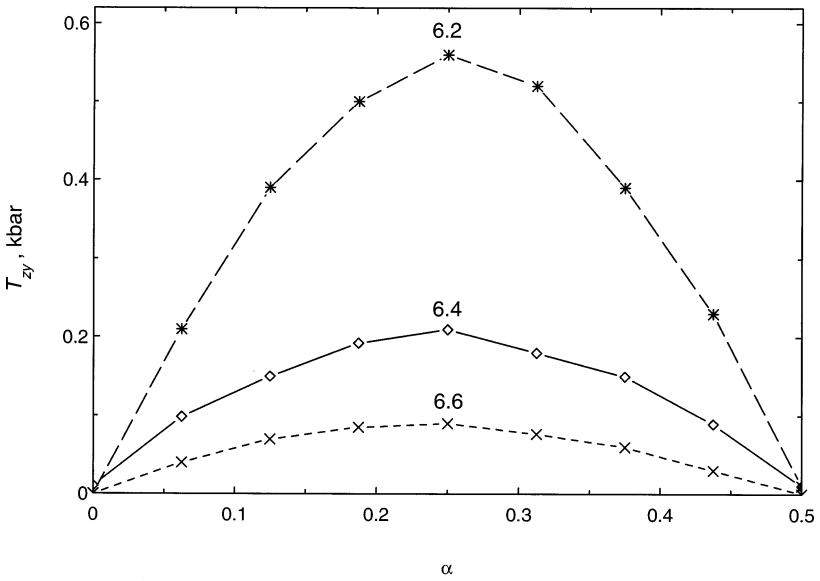

Figure 7. Shear stress in *y*-direction as a function of registry for a water monolayer confined between parallel graphite sheets. The numbers above the curves refer to the wall-to-wall separation in angstroms.

models failed to meet the adopted requirement for the sign and magnitude of the water−graphite interfacial tension γ_{sl}. The estimate of γ_{sl} as $\gamma(h)/2$ at $h = 40$ Å proved to be as low as −217 dyn/cm for model 1S and −107 dyn/cm for model 3Sa; i.e., both model surfaces were too hydrophilic. In an attempt to meet all the requirements for the water−graphite model potential, including the ability to reproduce the MP2 prediction for ΔE, we tested shorter ranged atom−atom potential functions, particularly for the H···C interaction. With increasing exponents *m* and *n*, the orientational dependence of the model potential became stronger, and the contribution of the second hydration layer to the total water−wall interaction energy decreased. This allowed us to reduce γ_{sl} while keeping ΔE equal to its MP2 estimate. For model 3Sb, whose parameters are listed in Table 1, the water−graphite interfacial tension γ_{sl} was found to be 32 dyn/cm. At wall-to-wall separations *h* corresponding to a compressed monolayer film ($h < 6.9$ Å, see the respective P_N in Figure 6), no cavitation of confined water was observed. The ratio T^c_{zy}/P_N did not exceed 0.07 at all separations tried. The effect of the 3Sb model wall on the density distribution of adjacent water can be judged from the density profile in Figure 4. Compared to the 3Sa model, the 3Sb model wall generates substantially lower density maxima, which can be expected for a more hydrophobic wall. The orientational distribution of water molecules next to the 3Sb wall was similar to that for the 3Sa wall (see Figure 3b), except that the occurrence of molecules with their OH bonds oriented toward the wall (i.e., with θ close to 180°) was more than 2 times higher.

4. Conclusions

The simulation results described in the previous section demonstrate convincingly that the thermodynamics and structure of the water−graphite interfacial region are extremely sensitive to the range and orientation dependence of the water−graphite interaction. The shorter the range and the stronger the orientation dependence, the more hydrophobic is the model graphite surface. The water−graphite binding energy ΔE, which characterizes the interaction strength of a *single* water molecule with graphite, is not, in any approximation, to be regarded as a measure for the water affinity of graphite. For a fixed ΔE, the water−

graphite interfacial tension γ_{sl} may vary over a very wide range and may even change the sign, depending on the analytical form assumed for the model potential. Equally significant is the effect of the form of the water−graphite model potential on the water structure in the interfacial region. Thus, a change from 1S- to 3S-type potentials may strongly affect the water density in the first hydration layer, whereas the preferred orientation of water molecules may even be reversed. All this calls into question the recent MD results that predict unusual dynamics and structuring of water inside CNT.[11−13]

Of the three water−graphite interaction models tested in this work, only the 3Sb one complies with both the MP2 calculation results and the experiment-based condition of a limited water affinity of graphite. Taking into account a great deal of arbitrariness involved in our parametrizations, it remains to be seen how well the 3Sb model describes the true water−graphite potential. In this respect, it would be highly desirable to extend the electronic structure calculations to at least two or three higher energy conformers of the water−graphite complex, such as conformers B and H in Figure 2.[47]

It is essential that the model potentials used in our simulations predict that the water monolayer compressed between two parallel graphite surfaces remains liquidlike and offers only slight resistance to shear. Considering the substantial differences in the range and orientational dependence between the three potentials, this result seems to be mainly associated with the geometry of the graphite lattice, viz., with its inability to be a template for an ordered packing of water molecules. Another important result of our simulations is the demonstration that a stable water monolayer can well exist between graphite surfaces even if the water−graphite interaction is slightly hydrophobic ($\gamma_{sl} > 0$). When coupled together, these results provide a better insight into the effect of water on the friction properties of graphite.

Acknowledgment. We are grateful to Prof. S. Granick for helpful remarks on the manuscript. This research was supported by the Deutsche Forschungsgemeinschaft and the Office for Naval Research.

References and Notes

(1) Erlanger, B. F.; Chen, B.-X.; Zhu, M.; Brus, L. *Nano Lett.* **2001**, *1*, 465−467.

(2) Huang, W.; Taylor, S.; Fu, K.; Lin, Y.; Zhang, D.; Hanks, T. W.; Rao, A. M.; Sun, Y.-P. *Nano Lett.* **2002**, *2* (4), 311−314.

(3) Balavoine, F.; Schultz, P.; Richard, C.; Mallouh, V.; Ebbesen, T. W.; Mioskowski, C. *Angew. Chem.* **1999**, *38* (13/14), 1912−1915.

(4) Sansom, M. S. P.; Biggin, P. C. *Nature* **2001**, *414*, 156−159.

(5) Lancaster, J. K. *Tribology Int.* **1990**, *23* (6), 371−89.

(6) Zaïdi, H.; Paulmier, D.; Lepage, J. *Appl. Surf. Sci.* **1990**, *44*, 221−233.

(7) Müller, E. A.; Rull, L. F.; Vega, L. F.; Gubbins, K. E. *J. Phys. Chem.* **1996**, *100* (4), 1189−1196.

(8) Werder, T.; Walther, J. H.; Jaffe, R. L.; Halicioglu, T.; Koumoutsakos, P. *J. Phys. Chem. B* **2003**, *107* (6), 1345−1352.

(9) Walther, J. H.; Jaffe, R.; Halicioglu, T.; Koumoutsakos, P. *J. Phys. Chem. B* **2001**, *105* (41), 9980−9987.

(10) Werder, T.; Walther, J. H.; Jaffe, R.; Halicioglu, T.; Noca, F.; Koumoutsakos, P. *Nano Lett.* **2001**, *1* (12), 697−702.

(11) Hummer, G.; Rasaiah, J. C.; Noworyta, J. P. *Nature* **2001**, *414*, 188−190.

(12) Koga, K.; Gao, G. T.; Tanaka, H.; Zeng, X. C. *Nature* **2001**, *412*, 802−805.

(13) Noon, W. H.; Ausman, K. D.; Smalley, R. E.; Ma, J. *Chem. Phys. Lett.* **2002**, *355*, 445−448.

(14) Marković, N.; Andersson, P. U.; Någård, M. B.; Petterson, J. B. C. *Chem. Phys.* **1999**, *247*, 413−430. Tomsic, A.; Marković, N.; Petterson, J. B. C. *Phys. Chem. Chem. Phys.* **2001**, *3*, 3667−3671.

(15) Bojan, M. J.; Steele, W. A. *Langmuir* **1987**, *3* (6), 1123−1127.

(16) Brooks, B. R.; Bruccoleri, R. E.; Olafson, B. D.; States, D. J.; Swaminathan, S.; Karplus, M. *J. Comput. Chem.* **1983**, *4* (2), 187−217.

(17) Cornell, W. D.; Cieplak, P.; Bayly, C. I.; Gould, I. R.; Merz, K. M., Jr.; Ferguson, D. M.; Spellmeyer, D. C.; Fox, T.; Caldwell, J. W.; Kollman, P. A. *J. Am. Chem. Soc.* **1995**, *117*, 5179−5197.

(18) Feller, D.; Jordan, K. D. *J. Phys. Chem. A* **2000**, *104* (44), 9971−9975.

(19) Vernov, A.; Steele, W. A. *Langmuir* **1992**, *8*, 155.

(20) Gale, R. L.; Beebe, R. A. *J. Phys. Chem.* **1964**, *68*, 555.

(21) Luna, M.; Colchero, J.; Baró, A. M. *J. Phys. Chem. B* **1999**, *103*, 9576−9581.

(22) Schrader, M. E. *J. Phys. Chem.* **1980**, *84*, 2774−2779.

(23) Morcos, I. *J. Chem. Phys.* **1972**, *57* (4), 1801−1802.

(24) Fowkes, F. M.; Harkins, W. D. *J. Am. Chem. Soc.* **1940**, *62* (12), 3377−3377.

(25) Hayashi, T.; Pertsin, A. J.; Grunze, M. *J. Chem. Phys.* **2002**, *117* (13), 6271−6280.

(26) Pertsin, A. J.; Kitaigorodsky, A. I. *The Atom-Atom Potential Method*; Springer-Verlag: Berlin, 1987.

(27) Kaplan, I. G. *Theory of Molecular Interactions*; Elsevier: Amsterdam, 1986.

(28) Allen, M. P.; Tildesley, D. J. *Computer Simulation of Liquids*; Clarendon Press: Oxford, UK, 1987.

(29) Benedict, L. X.; Chopra, N. G.; Cohen, M. L.; Zettl, A.; Louie, S. G.; Crespi, V. H. *Chem. Phys. Lett.* **1998**, *286*, 490−496.

(30) Jaffe, R. L. Technical report, NASA Ames Reseach Center, 2001.

(31) Jorgensen, W. L.; Chandrasekhar, J.; Madura, J. D.; Impey, R. W.; Klein, M. L. *J. Chem. Phys.* **1983**, *79*, 926.

(32) Lee, S. H.; Rossky, P. J. *J. Chem. Phys.* **1994**, *100* (4), 3334−3345.

(33) Crowell, A. D. *J. Chem. Phys.* **1958**, *29*, 448.

(34) Pertsin, A. J.; Grunze, M. *Langmuir* **2000**, *16* (23), 8223−8241.

(35) Pertsin, A. J.; Hayashi, T.; Grunze, M. *J. Phys. Chem. B* **2000**, *106* (47), 12274−12281.

(36) Stapleton, M. R.; Panagiotopoulos, A. *J. Chem. Phys.* **1990**, *92*, 1285.

(37) Swendsen, R. H.; Wang, J.-S. *Phys. Rev. Lett.* **1987**, *58*, 86.

(38) Irving, J. H.; Kirkwood, J. G. *J. Chem. Phys.* **1950**, *18* (6), 817−829.

(39) Bordarier, P.; Schoen, M.; Fuchs, A. H. *Phys. Rev. E* **1998**, *57* (2), 1621−1635.

(40) Schoen, M.; Gruhn, T.; Diestler, D. J. *J. Chem. Phys.* **1998**, *109* (1), 301−311.

(41) Curry, J. E. *J. Chem. Phys.* **2000**, *113* (6), 2400−2406.

(42) Diestler, D. J.; Schoen, M. *Phys. Rev. E* **2000**, *62* (5), 6615−6627.

(43) Persson, B. N. J. *Phys. Rev. B* **1993**, *48*, 18140.

(44) Lupkowski, M.; van Swol, F. *J. Chem. Phys.* **1991**, *95*, 1995.

(45) Gao, J.; Luedtke, W. D.; Landman, U. *J. Phys. Chem. B* **1998**, *102* (26), 5033−5037.

(46) Bhushan, B.; Israelachvili, J. N.; Landman, U. *Nature* **1995**, *374*, 607−615.

(47) A careful analysis of the accuracy of the MP2 calculations by Feller and Jordan[18] seems to be desirable as well. According to the recent publication by Karapetian and Jordan,[48] which appeared after the above-described GCMC simulations were completed, the value of ΔE found in ref 18 is most likely overestimated in magnitude as a consequence of a large uncertainty associated with the removal of the basis set superposition error. To appreciate the effect of a decrease in $|\Delta E|$ on the behavior of our 3S models, we made simulations with halved potential well depths ϵ_{OC} and ϵ_{HC}, which corresponded to $\Delta E = -2.9$ kcal/mol. As expected, the water affinity of the model surfaces reduced. As a consequence, the 3Sb model proved to be too hydrophobic: When confined between two parallel 3Sb model graphite sheets, a water monolayer experienced capillary evaporation. On the other hand, halving the potential well depths for the 3Sa model changed the sign of γ_{sl}, while the graphite sheets remained capable of holding the water monolayer. That is, the scaled 3Sa model satisfied all the conditions we imposed on the water−graphite potential.

(48) Karapetian, K.; Jordan, K. D. Properties of Water Clusters on a Graphite Sheet. In *Water in Confining Geometries*; Buch, V., Devlin, J. P., Eds.; Springer-Verlag: Berlin, Heidelberg, 2003; pp 139−150.